Hexagonal spin lattice with ferromagnetic intrachain and antiferromagnetic interchain couplings in an external magnetic field

E. Rastelli and A. Tassi

Dipartimento di Fisica, Università di Parma, 43100 Parma, Italy

(Received 26 August 1993)

The hexagonal Heisenberg model, in which the spins along the c axis interact via a ferromagnetic exchange coupling and those in the c plane via an antiferromagnetic one, undergoes nontrivial changes when an external magnetic field is applied in the c plane. In the classical approximation this model has the same phenomenology as the two-dimensional planar triangular antiferromagnet: it is characterized by infinitely many minimum-energy configurations, thermal fluctuations select one configuration out of the manifold, and an intermediate collinear phase intervenes between the low-field 120° three-sublattice configuration and the high-field asymmetric fan phase. We find that the quantum nature of the model leads to first-order phase transitions between the helix and fan phase and between the fan and saturated phase. This model is suitable to describe CsCuCl₃ and agreement between theoretical expectations and experiment is found.

I. INTRODUCTION

The two-dimensional (2D) triangular planar[1-3] and classical Heisenberg[4] antiferromagnets show a rich phase diagram when an external magnetic field H is applied in the plane. Indeed analytic low-temperature expansions and Monte Carlo (MC) calculations evidentiate four different configurations at increasing H for sufficiently low temperatures. Such phases are a distorted 120° three sublattice phase (with a spin opposite to the field), the "up-up-down" phase with two spins parallel and one antiparallel to the field, an asymmetric fan (with two spins parallel to each other, but not one directed along the field), and, finally, the saturated phase (with all spins parallel to the field). A unique property of the triangular planar and classical Heisenberg antiferromagnets is that at zero temperature infinitely many minimum-energy configurations exist even in the presence of an external applied magnetic field. These configurations correspond to the infinitely many spin patterns that in each elementary triangle satisfy the condition $S_1 + S_2 + S_3 - \mu H/6JS = 0$ where μ is the magnetic moment of a site and J is the spin-spin antiferromagnetic interaction. This degeneracy is lifted by thermal fluctuations which, at low temperatures, select the configuration with one spin antiparallel to the field.[1-3] Analytic expansions in $1/S$ show that the degeneracy of the ground state is lifted also in the 2D quantum triangular Heisenberg antiferromagnet[5] owing to the zero-point motion energy. Quantum fluctuations are also responsible for the stabilization of the "up-up-down" phase over a finite range of magnetic fields. The elementary excitation energies have been given for both the triangular planar antiferromagnet[3] and for the triangular Heisenberg antiferromagnet.[6] An interesting behavior of the uniform mode energies as a function of the external magnetic field is found for the Heisenberg model when the effect of an easy plane exchange anisotropy is accounted for.[6] The

behavior of the uniform modes as function of the magnetic field is strongly dependent on the ground state selected by quantum fluctuations. In particular, the uniform modes selected by quantum fluctuations compare favorably with magnetic resonance data[7,8] of CsCuCl₃, an ABX_3 compound with spin $S = 1/2$ where ferromagnetic chains parallel to the c axis are weakly coupled antiferromagnetically in the c plane where spins are located on a triangular lattice. The uniform magnetization of CsCuCl₃ has been measured as function of an external magnetic field applied both parallel and perpendicular to the c axis.[9] When the field is applied in the c plane the magnetization shows a plateau at a field about one-third of the saturation field and the value of the magnetization at the plateau is roughly one-third of its saturation value. The fit between the theoretical results obtained from the 2D triangular Heisenberg antiferromagnet and the experimental data of CsCuCl₃ is exciting[6] even though such a good fit could be an accident since the 3D nature of the actual compound is neglected. Here we study the 3D hexagonal Heisenberg model with ferromagnetic exchange coupling along the c axis and antiferromagnetic coupling in the c plane in order to keep the relevant features necessary to account for the magnetic properties of CsCuCl₃. We find that the classical version of this model shows the same peculiarities of the triangular antiferromagnet, for instance, infinitely many minimum-energy configurations in external magnetic field and selection of one particular configuration by thermal fluctuations.

Linearized equations of motion for the spin deviation operators provide the spin wave frequencies. The field dependence of these frequencies is strictly related to the minimum-energy configuration assumed. The zero-point motion energy which involves a sum over these frequencies is in its turn dependent on the minimum-energy configuration assumed, so that it is able to select one out of the infinite manifold of these configurations. At variance with classical models, in this quantum model the

selection of a particular configuration occurs at zero temperature. The minimum-energy configuration selected by quantum fluctuations is the same as that selected by thermal fluctuations at finite temperature. Anyway a significant effect of quantum fluctuations is the stabilization of an intermediate phase between the low-field distorted helix configuration shown in Fig. 1(a) and the high-field asymmetric fan configuration shown in Fig. 1(b) over a *finite* range of magnetic fields. On the contrary, this range shrinks to zero in the classical model for vanishing temperatures.

We find that the uniform mode frequencies of the low-field configuration compare favorably with magnetic resonance data of CsCuCl$_3$.[7,8] The intermediate phase stabilized by quantum fluctuations occurs for fields around one-third of the saturation field and is characterized by a magnetization one-third of its saturation value. Moreover, a plateau is found by a Maxwell construction that eliminates unphysical states with decreasing magnetization at increasing magnetic field. This should explain the plateau observed experimentally.[9] Note that the intermediate phase we find is a coexistence region between the distorted helix and the asymmetric fan phase. This is a relevant difference with respect to the the intermediate phase of the classical triangular antiferromagnet stabilized by thermal fluctuations.[1–4] Indeed, in the classical 2D models the intermediate phase is a homogeneous "up-up-down" phase with two spins parallel and one spin antiparallel to the field as shown in Fig. 1(b).

The format of the paper is the following: In Sec. II we study the minimum-energy configurations of the model in classical approximation and the spin wave dispersion curves obtained by linearized equations of motion of the spin operators. In Sec. III we consider the effect of quantum fluctuations on the ground state configuration and on the magnetization. Comparison with experimental data of CsCuCl$_3$ is given in Sec. IV. Finally, summary and conclusions are contained in Sec. V. Technical de-
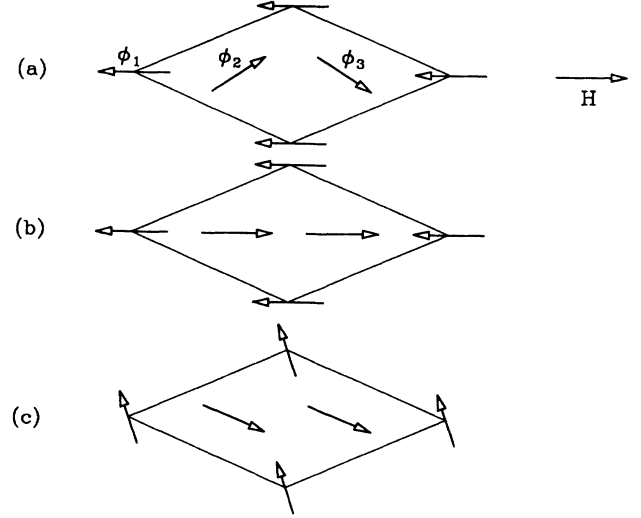
FIG. 1. The magnetic cell in a generic c plane of the hexagonal quantum Heisenberg antiferromagnet: (a) distorted helix phase for $h = 0.5$, (b)"up-up-down" phase for $h = 1$, (c) asymmetric fan phase for $h = 1.5$.

tails of the spin wave theory for the hexagonal lattice we consider are given in the Appendix.

II. GROUND STATE CONFIGURATION, SPIN WAVES, AND ZERO-POINT MOTION ENERGY

We consider a hexagonal lattice of ferromagnetic chains coupled by weak antiferromagnetic interaction. Figure 1 shows the $\sqrt{3} \times \sqrt{3}$ magnetic cell in a generic c plane. We assume the external magnetic field directed along a line of in-plane nearest neighbors. The Hamiltonian we consider reads

$$\mathcal{H} = -J_0 \sum_{i\delta'} \left(\mathbf{S}_i^{(a)} \cdot \mathbf{S}_{i+\delta'}^{(a)} + \mathbf{S}_i^{(b)} \cdot \mathbf{S}_{i+\delta'}^{(b)} + \mathbf{S}_i^{(c)} \cdot \mathbf{S}_{i+\delta'}^{(c)} \right) + \eta_0 J_0 \sum_{i\delta'} \left(S_i^{(a)z} S_{i+\delta'}^{(a)z} + S_i^{(b)z} S_{i+\delta'}^{(b)z} + S_i^{(c)z} S_{i+\delta'}^{(c)z} \right)$$

$$+ 2J \sum_{i\delta} \left(\mathbf{S}_i^{(a)} \cdot \mathbf{S}_{i+\delta}^{(b)} + \mathbf{S}_i^{(b)} \cdot \mathbf{S}_{i+\delta}^{(c)} + \mathbf{S}_i^{(c)} \cdot \mathbf{S}_{i+\delta}^{(a)} \right) - 2\eta J \sum_{i\delta} \left(S_i^{(a)z} S_{i+\delta}^{(b)z} + S_i^{(b)z} S_{i+\delta}^{(c)z} + S_i^{(c)z} S_{i+\delta}^{(a)z} \right)$$

$$- g\mu_B H \sum_i \left(S_i^{(a)x} + S_i^{(b)x} + S_i^{(c)x} \right), \tag{2.1}$$

where $2J_0$ is the ferromagnetic intrachain exchange interaction, $2J$ is the in-plane antiferromagnetic exchange interaction, $\eta_0, \eta > 0$ are the easy-plane exchange anisotropy that couple spins along the c axis and in the c plane, respectively. H is the external magnetic field, g is the Landé factor, μ_B is the Bohr magneton. i labels the sites of each one of the three sublattices labeled by a, b, c in which the hexagonal lattice is divided. $\delta' = (0, 0, \pm c)$ joins a spin with its intrachain nearest neighbors, $\delta = (a, 0, 0)$, $(-\frac{1}{2}a, \pm\frac{\sqrt{3}}{2}a, 0)$ joins a spin with its in-plane nearest neighbors.

We use the standard spin wave approach to obtain the ground state energy, the elementary excitation en-

ergy, and the low-temperature properties. We account for a configuration with three spins per unit cell, ϕ_1, ϕ_2, ϕ_3 being the angles between the spins of the a, b, c sublattices and the external magnetic field, respectively. Transformation to sublattice quantization axis, Holstein-Primakoff spin-boson transformation, minimization of the classical energy of the model (proportional to S^2) with respect to ϕ_1, ϕ_2, ϕ_3, truncation of the bosonic Hamiltonian within bilinear contribution and diagonalization of the so obtained harmonic Hamiltonian are given in the Appendix. Here we limit ourselves to show the main results.

Hamiltonian (2.1) is replaced by

$$\mathcal{H} = E_0 + \mathcal{H}_2. \tag{2.2}$$

E_0 is the ground state energy of the model in classical approximation $(S \to \infty)$

$$E_0 = 2JNS^2[\cos(\phi_1 - \phi_2) + \cos(\phi_2 - \phi_3) + \cos(\phi_3 - \phi_1)$$
$$- h(\cos\phi_1 + \cos\phi_2 + \cos\phi_3)] - 2J_0NS^2, \tag{2.3}$$

where $h = g\mu_B H/6JS$. Minimization of E_0 with respect to ϕ_1, ϕ_2, ϕ_3 gives the minimum-energy configuration in classical approximation. We obtain

$$\phi_1 = \phi, \quad \phi_2 = \phi_\mp, \quad \phi_3 = \phi_\pm, \tag{2.4}$$

where

$$\cos\phi_\mp = \frac{1}{2}\left[h - \cos\phi \mp \sin\phi\sqrt{\frac{3 - h^2 + 2h\cos\phi}{1 + h^2 - 2h\cos\phi}}\right], \tag{2.5}$$

$$\sin\phi_\mp = \frac{1}{2}\left[-\sin\phi \mp (h - \cos\phi)\sqrt{\frac{3 - h^2 + 2h\cos\phi}{1 + h^2 - 2h\cos\phi}}\right] \tag{2.6}$$

with $-\phi_M < \phi < \phi_M$ where $\phi_M = \pi$ for $0 \leq h \leq 1$, $\phi_M = \cos^{-1}(\frac{h^2-3}{2h})$ for $1 \leq h \leq 3$. This configuration coincides with that obtained for the triangular planar antiferromagnet[1-3] and for the triangular classical Heisenberg antiferromagnet.[4,6] As it is well known[1-3] the angle that the spins of one sublattice make with the field is arbitrary. This corresponds to an infinite degeneracy of the minimum-energy configuration which reads

$$E_0 = -JNS^2(3 + h^2) - 2J_0NS^2. \tag{2.7}$$

For $h \geq 3$ the classical minimum-energy configuration is nondegenerate and corresponds to the saturated phase $\phi_1 = \phi_2 = \phi_3 = 0$:

$$E_0 = -6JNS^2(h - 1) - 2J_0NS^2. \tag{2.8}$$

By a suitable Bogoliubov transformation given in the Appendix we obtain

$$\mathcal{H}_2 = \Delta E + \sum_{\mathbf{q}}\left(\hbar\omega_{\mathbf{q}}^{(1)}\alpha_{\mathbf{q}}^\dagger\alpha_{\mathbf{q}} + \hbar\omega_{\mathbf{q}}^{(2)}\beta_{\mathbf{q}}^\dagger\beta_{\mathbf{q}} + \hbar\omega_{\mathbf{q}}^{(3)}\sigma_{\mathbf{q}}^\dagger\sigma_{\mathbf{q}}\right), \tag{2.9}$$

where $\alpha_{\mathbf{q}}$, $\beta_{\mathbf{q}}$, $\sigma_{\mathbf{q}}$, are the destruction operators of the spin waves of wave vector $\mathbf{q}$. The spin wave energies are given by

$$\hbar\omega_{\mathbf{q}}^{(s)} = 4J_0S\sqrt{x^{(s)}}, \quad s = 1, 2, 3, \tag{2.10}$$

where $x^{(s)}$ are the solutions of the following cubic equation:

$$x^3 - ax^2 + bx - c = 0 \tag{2.11}$$

with a, b, c, given in the Appendix. The zero-point motion energy ΔE is given by
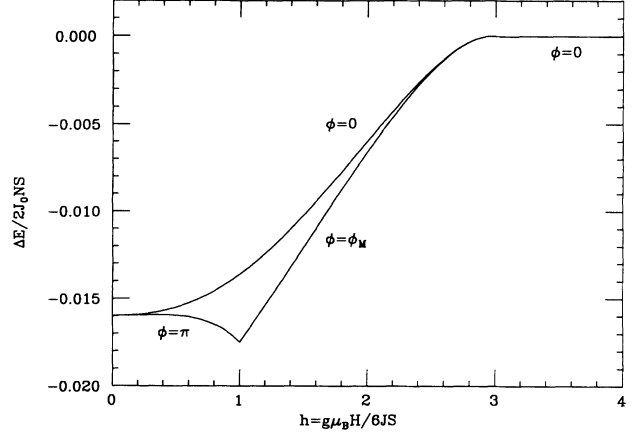
FIG. 2. Zero-point motion energy $\Delta E/2J_0NS$ vs magnetic field for $\eta_0 = 0$, $\eta = 0.054$, and $j = 0.263$. The upper curve corresponds to the choice $\phi = 0$, the lower curve (the stable configuration) to $\phi = \phi_M$.

$$\Delta E = -3JNS - 2J_0NS + \frac{1}{2}\sum_{s=1}^{3}\sum_{\mathbf{q}}\hbar\omega_{\mathbf{q}}^{(s)} \tag{2.12}$$

for $0 \leq h \leq 3$ and

$$\Delta E = -3JNS(h - 2) - 2J_0NS + \frac{1}{2}\sum_{s=1}^{3}\sum_{\mathbf{q}}\hbar\omega_{\mathbf{q}}^{(s)} \tag{2.13}$$

for $h \geq 3$. The ground state energy in the harmonic approximation is $E_G = E_0 + \Delta E$. For $0 \leq h \leq 3$ the ϕ dependence of the ground state energy is entered by ΔE. In particular, the last term of (2.12) is ϕ dependent since the spin wave frequencies $\omega_{\mathbf{q}}^{(s)}$ are ϕ dependent (see the Appendix). Numerical evaluation of ΔE as a function of ϕ gives the following result: ΔE is maximum for $\phi = 0$ and minimum for $\phi = \phi_M$. In Fig. 2 we show the minimum and maximum value of ΔE versus field for $\eta_0 = 0$, $\eta = 0.054$, and $j = \frac{3J}{2J_0} = 0.263$, a choice of parameters proper to model CsCuCl$_3$. For $0 < h < 1$ the stable configuration corresponds to $\phi = \pi$ and is shown in Fig. 1(a) (distorted helix). For $h = 1$ the stable configuration is given by Fig. 1(b) ("up-up-down" phase). For $1 < h < 3$ the stable configuration is characterized by $\phi = \phi_M$ and is shown in Fig. 1(c) (asymmetric fan). For $h \geq 3$ the saturated phase is the stable one.

III. FIRST-ORDER PHASE TRANSITION INDUCED BY QUANTUM FLUCTUATIONS

The free energy in harmonic approximation reads

$$F = E_0 + \Delta E + k_BT\sum_{s=1}^{3}\sum_{\mathbf{q}}\ln\left(1 - e^{-\beta\hbar\omega_{\mathbf{q}}^{(s)}}\right). \tag{3.1}$$

For $0 \leq h \leq 3$ we have

E. RASTELLI AND A. TASSI
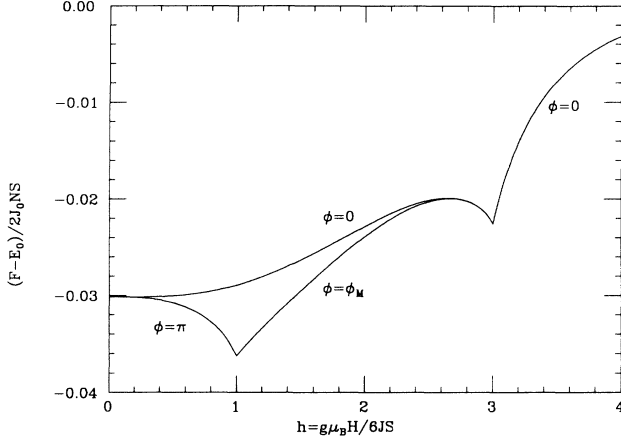
FIG. 3. Quantum and thermal contribution to the free energy $(F - E_0)/2J_0NS$ at $T = 10$ K for the same parameters as in Fig. 2.

$$F = -2J_0NS^2\left\{1 + j\left(1 + \frac{1}{3}\right) + \frac{1}{3S}\left[3(1+j) - f(t)\right]\right\},$$
$$(3.2)$$

where $t = \frac{k_BT}{4J_0S}$ and

$$f(t) = \frac{1}{\pi^3}\int_0^\pi dx \int_0^\pi dy \int_0^\pi dz$$
$$\times \sum_{s=1}^3\left[\sqrt{x^{(s)}} + 2t\ln\left(1 - e^{-\sqrt{x^{(s)}}/t}\right)\right]$$
$$(3.3)$$

with $x = \frac{3}{2}aq_x$, $y = \frac{\sqrt{3}}{2}aq_y$, $z = cq_z$. For $h \geq 3$

$$F = -2J_0NS^2\left\{1 + 2j(h - 1) + \frac{1}{3S}\left[3\right.\right.$$
$$\left.\left. +3j(h - 2) - f(t)\right]\right\}.$$
$$(3.4)$$

Like quantum fluctuations, thermal fluctuations are ϕ dependent for $0 < h < 3$, since $x^{(s)}$ are ϕ dependent in this range of fields. Again the stable configuration is characterized by $\phi = \phi_M$, as shown in Fig. 3, where a temperature $T = 10$ K is taken.

The magnetization is given by the usual thermodynamic realtion $M = -\frac{\partial F}{\partial H}$. If we define a reduced magnetization as $m = \frac{M}{g\mu_BNS}$ we have

$$m = \frac{1}{3}h - \frac{1}{6jS}\frac{\partial f(t)}{\partial h} \qquad (3.5)$$

for $0 \leq h \leq 3$ and

$$m = 1 + \frac{1}{2S} - \frac{1}{6jS}\frac{\partial f(t)}{\partial h} \qquad (3.6)$$

for $h \geq 3$.

Quantum fluctuations accounted for by the first term of Eq. (3.3) cause an interesting phenomenon in our model, that is the onset of two first-order phase transitions at about $h = 1$ and $h = 3$, respectively. Indeed, as shown in Fig. 2 by the lower curve, the zero-point motion energy is a function that decreases with field for $0 < h < 1$ and increases for $h > 1$. This means that the magnetization is higher than its classical value for $0 < h < 1$ and lower for $h > 1$ undergoing a discontinuous jump at $h = 1$. To avoid an unphysical decreasing of the magnetization at increasing magnetic field as involved by the jump, we make a Maxwell construction as shown in the inset of Fig. 4. At about $h = 1$ a coexistence region between the distorted helix and asymmetric fan phase replaces the discontinuity. The same can be done at $h = 3$ where a coexistence region between the asymmetric fan and saturated phase occurs. The temperature magnifies the plateau entered by the Maxwell construction as shown in Fig. 5. This behavior differs substantially from that of classical 2D models, where an intermediate new phase ("up-up-down" phase) between the low-field distorted helix and the high-field asymmetric fan is introduced by quantum fluctuations.[5] The "up-up-down"
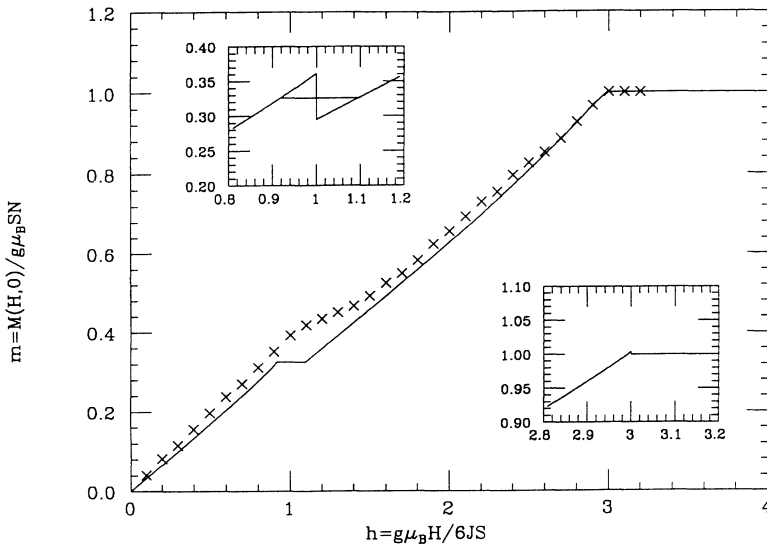
FIG. 4. Reduced magnetization vs magnetic field at $T = 0$ K for $\eta_0 = 0$, $\eta = 0.054$, and $j = 0.263$. The insets show the Maxwell construction at $h = 1$ (left, high) and $h = 3$ (right, low). Crosses are experimental data concerning CsCuCl$_3$ from Ref. 9.
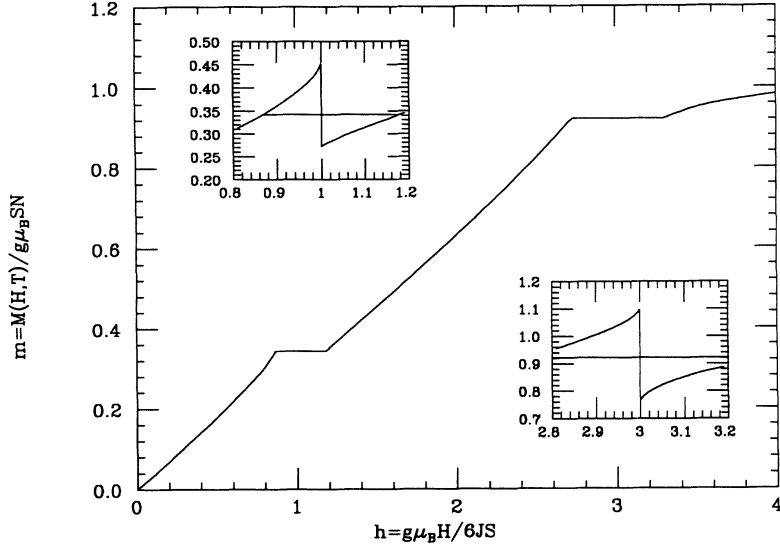
FIG. 5. Reduced magnetization vs magnetic field at $T = 10$ K for the same parameters as in Fig. 4.

phase, supported by thermal fluctuations in 2D classical triangular antiferromagnets, is a homogeneus phase with two spins pointing along the field and one spin pointing in the opposite direction [see Fig. 1(b)]. We think that the "up-up-down" phase in the 3D hexagonal quantum Heisenberg antiferromagnet should be replaced by a coexistence region between the distorted helix [Fig. 1(a)] and asymmetric fan [Fig. 1(c)] phase.

IV. MAGNETIC RESONANCE DATA AND MAGNETIZATION OF CsCuCl₃

Elastic neutron scattering experiment[10] allows the evaluation of the Hamiltonian parameters of Eq. (2.1) to fit CsCuCl₃, a hexagonal compound with $S = 1/2$ of the ABX_3 family, where A is an alkali element, B a magnetic ion, and X can be Cl, Br, or I. We can neglect the easy-plane exchange anisotropy along the c axis ($\eta_0 = 0$). The experiment gives $2J_0$=64.45 K=1342 GHz, $2J = 11.28$ K=235 GHz, $g = 2.19$. The fitting with magnetic resonance data[7] allows us to evaluate the easy-plane exchange anisotropy in the c plane: $\eta = 0.054$. Indeed, for $\eta_0 = 0$, $\mathbf{q} = 0$, and $0 \leq h \leq 3$ the solutions of (A14) lead to the following uniform mode frequencies:

$$\hbar\omega_0^{(1)} = 0, \qquad (4.1)$$

$$\hbar\omega_0^{(2)} = 6JS\left[\frac{3}{2}\eta + \frac{1}{2}(1 - \eta)h^2\right.$$

$$\left. -\frac{1}{2}h\sqrt{\eta\rho(h,\phi) + (1 - \eta)(h^2 - 4\eta)}\right]^{\frac{1}{2}}, \quad (4.2)$$

$$\hbar\omega_0^{(3)} = 6JS\left[\frac{3}{2}\eta + \frac{1}{2}(1 - \eta)h^2\right.$$

$$\left. +\frac{1}{2}h\sqrt{\eta\rho(h,\phi) + (1 - \eta)(h^2 - 4\eta)}\right]^{\frac{1}{2}} \quad (4.3)$$

with $\rho(h, \phi)$ given by (A19). In Fig. 6 we show the fitting for $\eta = 0.054$. The lower (upper) continuous curve is obtained taking $\phi = \phi_M$ in (4.2) [(4.3)]. The function of ϕ that appears in (4.2) and (4.3) is $\rho(h, \phi_M) = (h + 2)^2$ for $0 \leq h \leq 1$ and $\rho(h, \phi_M) = \frac{1}{2h^2}[(h^2-5)^2+2]$ for $1 \leq h \leq 3$. This choice corresponds to the minimum of the zero-point motion energy ΔE and the corresponding configurations are those shown in Fig. 1. Lower (upper) open circles are obtained taking $\phi = 0$ in (4.2) [(4.3)]. In this case one has $\rho(h, 0) = (h - 2)^2$ for $0 \leq h \leq 3$. This choice that corresponds to the maximum of ΔE leads to a configuration characterized by the spins of one sublattice pointing along the field and the spins of the other two sublattices symmetrically oriented with respect to the field. Incidentally, this configuration was originally assumed as the stable one to fit magnetic resonance data of CsCuCl₃.[7] The striking difference in the uniform mode energies versus field, depending on the choice of the ground state configuration, confirms the crucial role of quantum fluc-
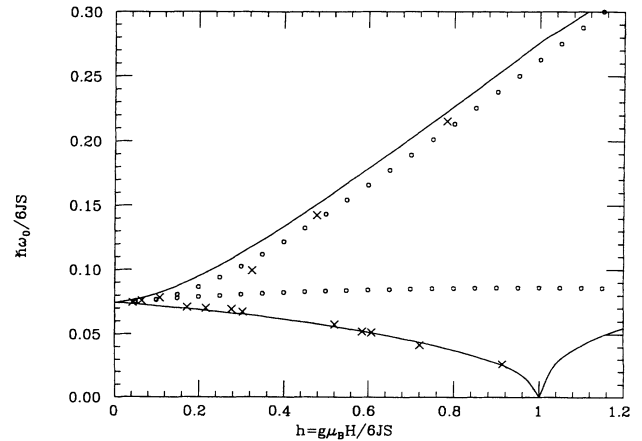
FIG. 6. Uniform mode frequencies of CsCuCl₃ vs magnetic field for $\eta_0 = 0$, $\eta = 0.054$, and $j = 0.263$. Continuous curves: $\phi = \phi_M$. Open circles: $\phi = 0$. Crosses: magnetic resonance data from Ref. 8.

tuations in selecting the configuration with $\phi = \phi_M$. For $h \geq 3$ the saturated phase is the stable configuration. The uniform mode frequencies become

$$\hbar\omega_0^{(1)} = \hbar\omega_0^{(2)} = 6JS\sqrt{(h-3)(h-3+\eta)}, \qquad (4.4)$$

$$\hbar\omega_0^{(3)} = 6JS\sqrt{h(h-2\eta)}. \qquad (4.5)$$

Experimental data concerning magnetization of $CsCuCl_3$ at $T = 1.1$ K (Ref. 9) compare favorably with our theoretical result at $T = 0$ K as shown in Fig. 4. In particular, the plateau at about $h = 1$ is in good agreement with the plateau observed at $H \simeq 11$ T. The plateau at $h = 3$ ($H \simeq 31$ T) is hard to be seen at so low temperatures. However, as shown in Fig. 5, the plateau are strongly affected by the temperature. In particular the plateau at $h = 3$ which is hardly detectable at $T = 0$ K is magnified at $T = 10$ K. Note that the Néel temperature of $CsCuCl_3$ at $H = 0$ is $T_N = 10.5$ K. For this reason we recommend magnetization measurements on $CsCuCl_3$ at a temperature higher than $T = 1.1$ K in order to test our theoretical interpretation of the properties of $CsCuCl_3$, when an external magnetic field is applied in the c plane.

The evaluation of the zero-point motion energy and magnetization in a way similar to ours has been performed when the external magnetic field is applied along the c axis.[11] In that case the magnetization is found to increase as the magnetic field increases, leading to a jump at $h = 1.08$ in qualitative agreement with experiment. Note that in our case (magnetic field applied perpendicular to the c axis) a plateau is found in the magnetization instead of a jump in agreement with experiment.

V. SUMMARY AND CONCLUDING REMARKS

We have discussed the magnetic properties of a hexagonal spin lattice of ferromagnetic chains parallel to the c axis weakly interacting via an antiferromagnetic interchain coupling when an external magnetic field is applied perpendicular to the c axis. This model is suitable for modeling some compounds of the ABX_3 family. In particular, we focus on $CsCuCl_3$ for which elastic neutron scattering,[10] magnetization,[9] and magnetic resonance data[7,8] as a function of the external magnetic field are available. Our approach consists of the linearization of the equation of motion of the spin deviation operators (spin wave theory) to obtain normal mode frequencies, quantum and thermal fluctuations (Secs. II and III). The model shows infinitely many minimum-energy configurations in classical approximation ($S \to \infty$) because the direction of one spin over three with respect to the external magnetic field is arbitrary. This peculiarity was already found in the 2D planar triangular antiferromagnet[1-3] and in the classical Heisenberg triangular antiferromagnet.[4] For these 2D classical models low-temperature expansions and MC simulations provide a rich phase diagram in the H-T plane, where a particular configuration is selected by thermal fluctuations. The possible configurations are (i) a distorted helix with a spin antiparallel

to the field, (ii) an "up-up-down" collinear phase, supported by crucial nonlinear effects, (iii) an asymmetric fan phase, and finally (iv) a saturated phase comes in for sufficiently high fields.

In our 3D model we find that quantum fluctuations select the same configuration as thermal fluctuations do in 2D classical models, but two first-order phase transitions between the distorted helix and the asymmetric fan configuration and between the asymmetric fan and the saturated phase are entered by a Maxwell construction that rules out unphysical states characterized by a decreasing magnetization at increasing magnetic field (Sec. III).

The magnetic resonance data[7,8] and the magnetization curve at low temperature[9] of $CsCuCl_3$ compare favorably with our theoretical results. In particular, the agreement is assured by the effect of quantum fluctuations that select the configuration with one spin opposite to the field at low fields (Sec. IV).

We suggest the opportunity of performing measurements of the magnetization versus field at higher temperatures in order to test the existence of another plateau in the vicinity of the saturation field. Also we urge neutron scattering measurements in order to establish the nature of the phase at $h \simeq 1$. Indeed, taking advantage from the geometrical factor in front of the strucure factor in the neutron cross section, one could check whether the plateau at $h = 1$ corresponds to a coexistence region of two phases (distorted helix and asymmetric fan phase) or it is due to the onset of a collinear "up-up-down" phase as occurs in the corresponding 2D classical models. In the former case the geometrical factor cannot reduce to zero the intensity of the magnetic Bragg's peaks, whereas in the latter, because of the collinear nature of the up-up-down phase, the choice of a proper geometry with the scattering wave vector parallel to the magnetization direction should reduce to zero the intensity of the elastic peaks.

APPENDIX

In this appendix we give some details of the spin wave approach to the model Hamiltonian (2.1). We introduce a local reference axis where ζ_i is the quantization axis of the spin at site i supposed to be the same for each spin belonging to the same sublattice. It is assumed to lay in the c plane (the easy plane). ϕ_1, ϕ_2, ϕ_3 are the angles that the local axes of the spins of the a, b, c sublattice make with the external magnetic field. For instance, for the a sublattice we have

$$\begin{aligned} S_i^{(a)x} &= -S_i^{(a)\eta}\sin\phi_1 + S_i^{(a)\zeta}\cos\phi_1, \\ S_i^{(a)y} &= S_i^{(a)\eta}\cos\phi_1 + S_i^{(a)\zeta}\sin\phi_1, \\ S_i^{(a)z} &= -S_i^{(a)\xi}. \end{aligned} \qquad (A1)$$

The customary Holstein-Primakoff spin-boson transformation

$$S_i^{(a)\xi} = \frac{\sqrt{2S}}{2}\left(a_i + a_i^\dagger + \cdots\right),$$

$$S_i^{(a)\eta} = \frac{\sqrt{2S}}{2i}\left(a_i - a_i^\dagger + \cdots\right), \qquad \text{(A2)}$$

$$S_i^{(a)\zeta} = S - a_i^\dagger a_i$$

and similar transformations for the b and c sublattices lead to the bosonic equivalent Hamiltonian

$$\mathcal{H} = E_0 + \mathcal{H}_1 + \mathcal{H}_2 + \cdots, \qquad \text{(A3)}$$

where all contributions with three or more Bose operators are neglected (harmonic approximation). a_i, b_i, c_i

are the usual destruction Bose operators of a spin deviation on a site i of the sublattice a, b, c, respectively. The ground state energy of the model in classical approximation $(S \to \infty)$ is

$$E_0 = 2JNS^2[\cos(\phi_1 - \phi_2) + \cos(\phi_2 - \phi_3) + \cos(\phi_3 - \phi_1)$$

$$-h(\cos\phi_1 + \cos\phi_2 + \cos\phi_3)] - 2J_0NS^2, \qquad \text{(A4)}$$

where $h = g\mu_B H/6JS$,

$$\mathcal{H}_1 = -6JS\left(\frac{\sqrt{2S}}{2i}\right)\sum_i \left\{\left[\sin(\phi_1 - \phi_2) + \sin(\phi_1 - \phi_3) - h\sin\phi_1\right](a_i - a_i^\dagger)\right.$$

$$\left. + \left[\sin(\phi_2 - \phi_3) + \sin(\phi_2 - \phi_1) - h\sin\phi_2\right](b_i - b_i^\dagger) + \left[\sin(\phi_3 - \phi_1) + \sin(\phi_3 - \phi_2) - h\sin\phi_3\right](c_i - c_i^\dagger)\right\}. \quad \text{(A5)}$$

Minimization of E_0 with respect to ϕ_1, ϕ_2, and ϕ_3 is equivalent to the condition $\mathcal{H}_1 = 0$. The angles between the spins belonging to the three sublattices and the field are explicitly given in Eqs. (2.4)–(2.6) of Sec. II as well as the classical minimum energy E_0 is given in Eqs. (2.7) and (2.8) of Sec. II. The bilinear Hamiltonian of Eq. (A3) becomes

$$\mathcal{H}_2 = \sum_\mathbf{q}\left\{6JS + 4J_0S\left[1 - \left(1 - \frac{1}{2}\eta_0\right)\cos(cq_z)\right]\right\}$$

$$\times(a_\mathbf{q}^\dagger a_\mathbf{q} + b_\mathbf{q}^\dagger b_\mathbf{q} + c_\mathbf{q}^\dagger c_\mathbf{q}) + \sum_\mathbf{q}\eta_0 J_0S\cos(cq_z)(a_\mathbf{q}a_{-\mathbf{q}} + a_\mathbf{q}^\dagger a_{-\mathbf{q}}^\dagger + b_\mathbf{q}b_{-\mathbf{q}} + b_\mathbf{q}^\dagger b_{-\mathbf{q}}^\dagger + c_\mathbf{q}c_{-\mathbf{q}} + c_\mathbf{q}^\dagger c_{-\mathbf{q}}^\dagger)$$

$$+ \sum_\mathbf{q}3JS\left\{\left[1 - \eta - \cos(\phi_1 - \phi_2)\right]\left(\gamma_\mathbf{q}^* a_\mathbf{q}b_{-\mathbf{q}} + \gamma_\mathbf{q}a_\mathbf{q}^\dagger b_{-\mathbf{q}}^\dagger\right) + \left[1 - \eta + \cos(\phi_1 - \phi_2)\right]\left(\gamma_\mathbf{q}^* a_\mathbf{q}b_\mathbf{q}^\dagger + \gamma_\mathbf{q}a_\mathbf{q}^\dagger b_\mathbf{q}\right)\right.$$

$$+ \left[1 - \eta - \cos(\phi_2 - \phi_3)\right]\left(\gamma_\mathbf{q}^* b_\mathbf{q}c_{-\mathbf{q}} + \gamma_\mathbf{q}b_\mathbf{q}^\dagger c_{-\mathbf{q}}^\dagger\right) + \left[1 - \eta + \cos(\phi_2 - \phi_3)\right]\left(\gamma_\mathbf{q}^* b_\mathbf{q}c_\mathbf{q}^\dagger + \gamma_\mathbf{q}b_\mathbf{q}^\dagger c_\mathbf{q}\right)$$

$$\left. + \left[1 - \eta - \cos(\phi_3 - \phi_1)\right]\left(\gamma_\mathbf{q}^* c_\mathbf{q}a_{-\mathbf{q}} + \gamma_\mathbf{q}c_\mathbf{q}^\dagger a_{-\mathbf{q}}^\dagger\right) + \left[1 - \eta + \cos(\phi_3 - \phi_1)\right]\left(\gamma_\mathbf{q}^* c_\mathbf{q}a_\mathbf{q}^\dagger + \gamma_\mathbf{q}c_\mathbf{q}^\dagger a_\mathbf{q}\right)\right\} \qquad \text{(A6)}$$

for $0 \leq h \leq 3$, and

$$\mathcal{H}_2 = \sum_\mathbf{q}\left\{6JS(h - 2) + 4J_0S\left[1 - \left(1 - \frac{1}{2}\eta_0\right)\cos(cq_z)\right]\right\}$$

$$\times(a_\mathbf{q}^\dagger a_\mathbf{q} + b_\mathbf{q}^\dagger b_\mathbf{q} + c_\mathbf{q}^\dagger c_\mathbf{q}) + \sum_\mathbf{q}\eta_0 J_0S\cos(cq_z)(a_\mathbf{q}a_{-\mathbf{q}} + a_\mathbf{q}^\dagger a_{-\mathbf{q}}^\dagger + b_\mathbf{q}b_{-\mathbf{q}} + b_\mathbf{q}^\dagger b_{-\mathbf{q}}^\dagger + c_\mathbf{q}c_{-\mathbf{q}} + c_\mathbf{q}^\dagger c_{-\mathbf{q}}^\dagger)$$

$$+ \sum_\mathbf{q}3JS\left[-\eta\left(\gamma_\mathbf{q}^* a_\mathbf{q}b_{-\mathbf{q}} + \gamma_\mathbf{q}a_\mathbf{q}^\dagger b_{-\mathbf{q}}^\dagger\right) + (2 - \eta)\left(\gamma_\mathbf{q}^* a_\mathbf{q}b_\mathbf{q}^\dagger + \gamma_\mathbf{q}a_\mathbf{q}^\dagger b_\mathbf{q}\right)\right.$$

$$\left. - \eta\left(\gamma_\mathbf{q}^* b_\mathbf{q}c_{-\mathbf{q}} + \gamma_\mathbf{q}b_\mathbf{q}^\dagger c_{-\mathbf{q}}^\dagger\right) + (2 - \eta)\left(\gamma_\mathbf{q}^* b_\mathbf{q}c_\mathbf{q}^\dagger + \gamma_\mathbf{q}b_\mathbf{q}^\dagger c_\mathbf{q}\right) - \eta\left(\gamma_\mathbf{q}^* c_\mathbf{q}a_{-\mathbf{q}} + \gamma_\mathbf{q}c_\mathbf{q}^\dagger a_{-\mathbf{q}}^\dagger\right) + (2 - \eta)\left(\gamma_\mathbf{q}^* c_\mathbf{q}a_\mathbf{q}^\dagger + \gamma_\mathbf{q}c_\mathbf{q}^\dagger a_\mathbf{q}\right)\right]$$

$$\text{(A7)}$$

for $h \geq 3$. The operators $a_\mathbf{q}$, $b_\mathbf{q}$, $c_\mathbf{q}$ are the spatial Fourier transforms of a_i, b_i, c_i. The structure factor $\gamma_\mathbf{q}$ is given by

$$\gamma_\mathbf{q} = \frac{1}{3}\left[e^{iaq_x} + 2e^{-i\frac{1}{2}aq_x}\cos\left(\frac{\sqrt{3}}{2}aq_y\right)\right]. \qquad \text{(A8)}$$

In order to diagonalize $\mathcal{H}_2$ we use the well-known tech-

nique of the equation of motion for the boson operators. We have

$$\hbar\omega_\mathbf{q}^{(1)}\alpha_\mathbf{q} = [\alpha_\mathbf{q}, \mathcal{H}_2], \quad \hbar\omega_\mathbf{q}^{(2)}\beta_\mathbf{q} = [\beta_\mathbf{q}, \mathcal{H}_2], \qquad \text{(A9)}$$

$$\hbar\omega_\mathbf{q}^{(3)}\sigma_\mathbf{q} = [\sigma_\mathbf{q}, \mathcal{H}_2],$$

where the following Bogoliubov transformations are assumed:

$$\alpha_{\mathbf{q}} = u_{\mathbf{q}}^{(1)}a_{\mathbf{q}} - v_{\mathbf{q}}^{(1)}a_{-\mathbf{q}}^{\dagger} + r_{\mathbf{q}}^{(1)}b_{\mathbf{q}} - s_{\mathbf{q}}^{(1)}b_{-\mathbf{q}}^{\dagger}$$
$$+ p_{\mathbf{q}}^{(1)}c_{\mathbf{q}} - q_{\mathbf{q}}^{(1)}c_{-\mathbf{q}}^{\dagger}, \tag{A10}$$

$$\beta_{\mathbf{q}} = u_{\mathbf{q}}^{(2)}a_{\mathbf{q}} - v_{\mathbf{q}}^{(2)}a_{-\mathbf{q}}^{\dagger} + r_{\mathbf{q}}^{(2)}b_{\mathbf{q}} - s_{\mathbf{q}}^{(2)}b_{-\mathbf{q}}^{\dagger}$$
$$+ p_{\mathbf{q}}^{(2)}c_{\mathbf{q}} - q_{\mathbf{q}}^{(2)}c_{-\mathbf{q}}^{\dagger}, \tag{A11}$$

$$\sigma_{\mathbf{q}} = u_{\mathbf{q}}^{(3)}a_{\mathbf{q}} - v_{\mathbf{q}}^{(3)}a_{-\mathbf{q}}^{\dagger} + r_{\mathbf{q}}^{(3)}b_{\mathbf{q}} - s_{\mathbf{q}}^{(3)}b_{-\mathbf{q}}^{\dagger}$$
$$+ p_{\mathbf{q}}^{(3)}c_{\mathbf{q}} - q_{\mathbf{q}}^{(3)}c_{-\mathbf{q}}^{\dagger}, \tag{A12}$$

$\alpha_{\mathbf{q}}$, $\beta_{\mathbf{q}}$, $\sigma_{\mathbf{q}}$ are the destruction operators of spin waves that diagonalize $\mathcal{H}_2$. Equations (A9) and those for the corresponding creation bose operators lead to a homogeneous system of six equations for the six unknowns $u_{\mathbf{q}}, v_{\mathbf{q}}, r_{\mathbf{q}}, s_{\mathbf{q}}, p_{\mathbf{q}}, q_{\mathbf{q}}$. Solutions exist only in correspondence of the zeros of the determinant of the system. These eigenvalues are the spin wave frequencies we are looking for. The result is

$$\hbar\omega_{\mathbf{q}}^{(s)} = 4J_0 S\sqrt{x^{(s)}}, \quad s = 1,2,3, \tag{A13}$$

where $x^{(s)}$ are the solutions of the following cubic equation:

$$x^3 - ax^2 + bx - c = 0, \tag{A14}$$

where, for $0 \le h \le 3$, one has

$$a = 3\big[1 - \cos(cq_z) + j\big]\big[1 - (1 - \eta_0)\cos(cq_z) + j\big] + 2j^2(1 - \eta)s_1|\gamma_{\mathbf{q}}|^2, \tag{A15}$$

$$b = \big[1 - (1 - \eta_0)\cos(cq_z) + j\big]^2\Big\{3\big[1 - \cos(cq_z) + j\big]^2 - s_2 j^2|\gamma_{\mathbf{q}}|^2\Big\}$$
$$+ (1 - \eta)j^2\big[1 - (1 - \eta_0)\cos(cq_z) + j\big]\Big\{2s_1\big[1 - \cos(cq_z) + j\big]|\gamma_{\mathbf{q}}|^2 + \frac{1}{2}j(s_2 - s_1^2)\big(\gamma_{\mathbf{q}}^3 + \gamma_{\mathbf{q}}^{*3}\big)\Big\}$$
$$+ (1 - \eta)^2 j^2\Big\{-3\big[1 - \cos(cq_z) + j\big]^2|\gamma_{\mathbf{q}}|^2 - s_1 j\big[1 - \cos(cq_z) + j\big]\big(\gamma_{\mathbf{q}}^3 + \gamma_{\mathbf{q}}^{*3}\big) + s_1^2 j^2|\gamma_{\mathbf{q}}|^4\Big\}, \tag{A16}$$

$$c = \Big\{\big[1 - \cos(cq_z) + j\big]^3 - s_2 j^2\big[1 - \cos(cq_z) + j\big]|\gamma_{\mathbf{q}}|^2 + \frac{1}{2}(s_2 - 1)j^3\big(\gamma_{\mathbf{q}}^3 + \gamma_{\mathbf{q}}^{*3}\big)\Big\}$$
$$\times\Big\{\big[1 - (1 - \eta_0)\cos(cq_z) + j\big]^3 - 3(1 - \eta)^2 j^2\big[1 - (1 - \eta_0)\cos(cq_z) + j\big]|\gamma_{\mathbf{q}}|^2 + (1 - \eta)^3 j^3\big(\gamma_{\mathbf{q}}^3 + \gamma_{\mathbf{q}}^{*3}\big)\Big\} \tag{A17}$$

with $j = \frac{3J}{2J_0}$

$$s_1 = -\frac{3}{2} + \frac{1}{2}h^2, \quad s_2 = \frac{3}{4} + \frac{1}{4}h^2\rho(h,\phi) \tag{A18}$$

$$\rho(h,\phi) = \frac{4 - 4h\cos\phi(4\cos^2\phi - 1) + h^2(16\cos^2\phi - 3) - 6h^3\cos\phi + h^4}{1 - 2h\cos\phi + h^2}. \tag{A19}$$

Notice the ϕ dependence of a, b, c. For $h \ge 3$, the coefficients of (A14) are given by

$$a = 3\big[1 - \cos(cq_z) + j(h - 2)\big]\big[1 - (1 - \eta_0)\cos(cq_z) + j(h - 2)\big] + 6j^2(1 - \eta)|\gamma_{\mathbf{q}}|^2, \tag{A20}$$

$$b = 3\big[1 - (1 - \eta_0)\cos(cq_z) + j(h - 2)\big]^2\Big\{\big[1 - \cos(cq_z) + j(h - 2)\big]^2 - j^2|\gamma_{\mathbf{q}}|^2\Big\}$$
$$+ 3(1 - \eta)j^2\big[1 - (1 - \eta_0)\cos(cq_z) + j(h - 2)\big]\Big\{2\big[1 - \cos(cq_z) + j(h - 2)\big]|\gamma_{\mathbf{q}}|^2 - j\big(\gamma_{\mathbf{q}}^3 + \gamma_{\mathbf{q}}^{*3}\big)\Big\}$$
$$+ 3(1 - \eta)^2 j^2\Big\{-\big[1 - \cos(cq_z) + j(h - 2)\big]^2|\gamma_{\mathbf{q}}|^2 - j\big[1 - \cos(cq_z) + j(h - 2)\big]\big(\gamma_{\mathbf{q}}^3 + \gamma_{\mathbf{q}}^{*3}\big) + 3j^2|\gamma_{\mathbf{q}}|^4\Big\}, \tag{A21}$$

$$c = \Big\{\big[1 - \cos(cq_z) + j(h - 2)\big]^3 - 3j^2\big[1 - \cos(cq_z) + j(h - 2)\big]|\gamma_{\mathbf{q}}|^2 + j^3\big(\gamma_{\mathbf{q}}^3 + \gamma_{\mathbf{q}}^{*3}\big)\Big\}$$
$$\times\Big\{\big[1 - (1 - \eta_0)\cos(cq_z) + j(h - 2)\big]^3$$
$$- 3(1 - \eta)^2 j^2\big[1 - (1 - \eta_0)\cos(cq_z) + j(h - 2)\big]|\gamma_{\mathbf{q}}|^2 + (1 - \eta)^3 j^3\big(\gamma_{\mathbf{q}}^3 + \gamma_{\mathbf{q}}^{*3}\big)\Big\}. \tag{A22}$$

The diagonal form of $\mathcal{H}_2$ is given in Eq. (2.9) of Sec. II.

[1] H. Kawamura, J. Phys. Soc. Jpn. **53**, 2452 (1984).

[2] D. H. Lee, J. D. Joannopoulos, J. W. Negele, and D. P. Landau, Phys. Rev. Lett. **52**, 433 (1984); Phys. Rev. B **33**, 450 (1986).

[3] E. Rastelli, A. Tassi, A. Pimpinelli, and S. Sedazzari, Phys. Rev. B **45**, 7936 (1992).

[4] H. Kawamura and S. Miyashita, J. Phys. Soc. Jpn. **54**, 4530 (1985).

[5] A. V. Chubukov and D. I. Golosov, J. Phys. C **3**, 69 (1991).

[6] E. Rastelli and A. Tassi, Z. Phys. B (to be published).

[7] W. Palme, F. Mertens, O. Born, B. Lüthi, and U. Schotte, Solid State Commun. **76**, 873 (1990).

[8] W. Palme, H. Kriegelstein, G. Gojkovic, and B. Lüthi (unpublished).

[9] H. Nojiri, Y. Tokunaga, and M. Motokawa, J. Phys. (Paris) Colloq. **49**, C8-1459 (1988).

[10] Y. Tazuke, H. Tanaka, K. Iio, and K. Nagata, J. Phys. Soc. Jpn. **50**, 3919 (1981).

[11] H. Shiba and T. Nikuni, in *Recent Advances in Magnetism of Transition Metal Compounds*, edited by A. Kotani and N. Suzuki (World Scientific, Singapore, 1992).